The local space density of dwarf galaxies

Article (Published Version)

THE ASTROPHYSICAL JOURNAL, 489:29–36, 1997 November 1

THE LOCAL SPACE DENSITY OF DWARF GALAXIES

JON LOVEDAY
Department of Astronomy and Astrophysics, University of Chicago, 5640 S. Ellis Avenue, Chicago, IL 60637;
loveday@oddjob.uchicago.edu
Received 1997 March 5; accepted 1997 June 16

ABSTRACT

We estimate the luminosity function of field galaxies over a range of 10 mag ($-22 < M_{B_J} < -12$ for $H_0 = 100$ km s^{-1} Mpc^{-1}) by counting the number of faint APM galaxies around Stromlo-APM redshift survey galaxies at known distance. The faint end of the luminosity function rises steeply at $M_{B_J} \approx -15$, implying that the space density of dwarf galaxies is at least 2 times larger than predicted by a Schechter function with flat faint-end slope. Such a high abundance of dwarf galaxies at low redshift can help explain the observed number counts and redshift distributions of faint galaxies without invoking exotic models for galaxy evolution.

Subject headings: cosmology: observations — galaxies: distances and redshifts — galaxies: evolution — galaxies: luminosity function, mass function — surveys

1. INTRODUCTION

Knowledge of the space density of dwarf galaxies in the local universe is of great importance both in its own right, for example to constrain models of galaxy formation and to understand the local distribution of matter, and also in order to interpret observations of faint galaxies. For quite some time now (see, e.g., the review by Koo & Kron 1992), galaxy number counts, particularly in blue passbands, have been found to increase faster with apparent magnitude than predicted by simple no-evolution models, whereas the redshift distribution of galaxies in faint surveys *is* compatible with no evolution. Various models have been proposed to account for this discrepancy, including a disappearing or fading population of dwarf galaxies (Broadhurst, Ellis, & Shanks 1988; Cowie, Songaila, & Hu 1991; Babul & Rees 1992), nonconservation of galaxy numbers through merging (White 1989; Cowie et al. 1991; Broadhurst, Ellis, & Glazebrook 1992), or adoption of a nonzero cosmological constant (Fukugita et al. 1990). The automated plate measurement (APM) galaxy number counts of Maddox et al. (1990c) show counts at $b_J = 20.5$ a factor of 2 higher than expected from a no-evolution model, thus further exacerbating the discrepancy between observed number counts and redshift distributions.

Other authors, however (Koo & Kron 1992; Koo, Gronwall, & Bruzual 1993; Gronwall & Koo 1995), have suggested that modifying the assumptions going into the no-evolution models can help reconcile the observed number counts and redshift distributions, without resorting to exotic evolution models or nonstandard cosmologies. In particular, no-evolution models have traditionally assumed a Schechter (1976) form for the luminosity function with moderate faint-end slope, e.g., $\alpha = -1.25$ (Ellis 1987) or $\alpha = -1.15$ (Lilly 1993). Gronwall & Koo (1995) show that number counts in K, R, and B_J bands, as well as color and redshift distributions, are matched well by a no-evolution model in which the faint end of the galaxy luminosity function ($M_{B_J} \gtrsim -15$[1]) is dominated by blue galaxies ($B-V \leq 0.6$) and rises significantly above a Schechter function with flat faint-end slope. To date, there have been few measurements of the shape of the local field galaxy luminosity function at such low luminosities. Eales (1993) measured an apparent upturn in the luminosity function (LF) at $M_{B_J} \gtrsim -15$ for galaxies at $z < 0.1$. However, he used the $1/V_{\max}$ method to compute the LF, and so it is subject to bias due to an inhomogeneous distribution of a very small number of galaxies. A similar caution should be applied to the results of Lonsdale & Chokshi (1993), whose lowest-luminosity measurement is consistent with a flat faint-end Schechter function anyway due to Poisson statistics alone. The analysis by Marzke et al. (1994) of the CfA Redshift Survey shows evidence for an upturn in the LF at low luminosities, although the possibility of a scale error in the Zwicky magnitude system makes the amplitude of the faint-end excess uncertain (but see Takamiya & Kron 1995). Probably the best evidence for an upturn in the LF at low luminosities comes from a recent measurement of the galaxy luminosity function from the ESO Slice Project (Zucca et al. 1997), who find an excess of galaxies fainter than $M_{B_J} \approx -17$ above their best-fit Schechter function.

In this paper we push the measurement of the field galaxy luminosity function to fainter limits than previous work by counting the statistical excess of faint ($b_J < 20.5$) galaxies in the APM Galaxy Survey seen in projection around local galaxies at known distance in the Stromlo-APM Redshift Survey. The method by which we estimate the luminosity function is described in the following section. The galaxy samples and the application of the method are described in § 3 and in § 4 we justify the use of nearby center galaxies to measure the faint end of the galaxy LF. Results are presented in § 5, and several tests of our procedure are described in § 6. We conclude in § 7.

2. METHOD

Given a catalog containing positions and magnitudes for a large number of galaxies of unknown redshift and a smaller redshift survey in the same area of sky, one can measure the galaxy luminosity function to fainter luminosities than using the redshift survey alone. The technique used here to measure the abundance of dwarf galaxies relies on the assumption that correlated galaxies seen close in projection on the sky to a galaxy of known distance are also at the same distance. Although we do not know individually which galaxies are correlated, we can statistically determine the numbers of associated galaxies as a function of apparent

[1] Throughout, we assume a Hubble constant H_0 of 100 km s^{-1} Mpc^{-1}.

magnitude, and hence absolute magnitude. Repeating this for a large number of center galaxies, we can measure a luminosity function with good statistical accuracy at the faint end.

Perhaps the most straightforward approach is to count the excess number of galaxies in bins of absolute magnitude out to a fixed projected separation around each center galaxy, and to sum over center galaxies. This approach was employed by Phillipps & Shanks (1987), who counted the numbers of galaxies down to $b_J = 20.5$ from COSMOS scans of United Kingdom Schmidt Telescope (UKST) plates about center galaxies taken from various Durham redshift surveys, to measure the field galaxy LF over the magnitude range $-20.5 < M_{B_J} < -16$. However, as pointed out by Saunders et al. (1992) in a slightly different context, such an approach is not very efficient as center galaxies at small distances contribute little signal but a large number of galaxies to the sum, since nearby a fixed projected separation corresponds to a large solid angle, and so the excess neighbors are dominated by projection effects. For this reason, Phillipps & Shanks only used center galaxies at distances larger than 100 h^{-1} Mpc, thus limiting their ability to probe the faint end of the LF.

Here, we generalize the method of Saunders et al. (1992) to estimate a (noisy) LF for each center galaxy and then combine the LF estimates in a minimum-variance way. Saunders et al. counted galaxies in bins of projected separation σ about center galaxies of known redshift to estimate the projected correlation function, $\Xi(\sigma)$, which is related to the spatial correlation function, $\xi(r)$, by

$$\Xi(\sigma) = \int_{-\infty}^{+\infty} \xi(\sqrt{\Delta y^2 + \sigma^2}) d\Delta y \ . \quad (1)$$

We count galaxies as a function of σ and magnitude to estimate the quantity $X(M, \sigma) = \phi(M)\Xi(\sigma)$. Assuming a model for $\Xi(\sigma)$ then yields the luminosity function $\phi(M)$.

2.1. *Estimating $X(M, \sigma)$ from a Single Center Galaxy*

Consider a center galaxy at known distance y. We count the number of galaxies n in bins of projected separation $\sigma \pm \delta\sigma/2$ and apparent magnitude $m \pm \delta m/2$ about this center galaxy. The expected value of n is

$$\langle n \rangle = \frac{2\pi a \sin\theta\, \delta\sigma}{y} \int_0^\infty \phi[M(m, x)]\delta m x^2 [1 + \xi(r)] dx \ , \quad (2)$$

where $r^2 = x^2 + y^2 - 2xy\cos(\theta)$ is the square of the physical separation between galaxies at distance x and y with angular separation $\theta = \sigma/y$, a is the fraction of the projected annulus within the survey boundary and $\phi(M)\delta m$ is the number density of galaxies of absolute magnitude $M \pm \delta m/2$. The absolute magnitude M as a function of apparent magnitude m and distance x (in h^{-1} Mpc, with corresponding redshift z) is given by the usual formula: $M(m, x) = m - 5\log[x(1 + z)] - 25 - 3z$, where the final $-3z$ term is an approximate K-correction for galaxies of unknown type in the b_J passband.

For center galaxies at moderate distance y ($y \gg \sigma$ and $\xi(y) \ll 1$),

$$\langle n \rangle \approx \frac{2\pi a \sin\theta\, \delta\sigma}{y} [\bar{N}(m)\delta m + \phi[M(m, y)]\delta m y^2 \Xi(\sigma)] \ , \quad (3)$$

where $\bar{N}(m)\delta m$ is the surface density of galaxies of apparent magnitude $m \pm \delta m/2$ in the two-dimensional catalog.

As discussed by Saunders et al., this approximation is subject to biases due to the fact that for nearby galaxies, x^2 may grow faster than $\xi(r)$ falls off, and so excess pairs may not be close to the galaxy of known redshift. Conversely, at large distances, the selection function may be falling off so steeply that neighbors in projection will on average tend to be nearer than y. These biases are corrected for as discussed below.

To correct for the survey boundary, we count the number n_r of randomly distributed points of mean surface density $\bar{N}_r$ in the same σ bins. Scaling n_r to the surface density of galaxies of magnitude m, $n'(m, \sigma) = [\bar{N}(m)/\bar{N}_r]n_r(\sigma)$, we expect

$$\langle n' \rangle = \frac{2\pi a \sin\theta\, \delta\sigma}{y} \bar{N}(m)\delta m \ . \quad (4)$$

Our estimate of the relative excess $X(M, \sigma) = \phi(M)\Xi(\sigma)$ is then

$$X(M, \sigma) = \frac{1}{p(m, \sigma, y)} \left(\frac{n}{n'} - 1 \right) , \quad (5)$$

where

$$p(m, \sigma, y) = \frac{1}{\bar{N}(m)} k(m, \sigma, y) y^2 \ , \quad (6)$$

corrects for projection effects and the factor $k(m, \sigma, y)$ corrects for biases caused by the small angle/large distance approximation. From equation (2), the expectation value of X is

$$\langle X(M, \sigma) \rangle = \frac{1}{y^2 k(m, \sigma, y)} \int_0^\infty \phi[M(m, x)] x^2 \xi(r) dx \ , \quad (7)$$

and so setting

$$k(m, \sigma, y) = \frac{\int_0^\infty \phi[M(m, x)] x^2 \xi(r) dx}{y^2 \Xi(\sigma) \phi[M(m, y)]} \ , \quad (8)$$

will make $X(M, \sigma)$ an unbiased estimate of $\phi(M)\Xi(\sigma)$. Our estimator for $\phi(M)$ thus depends on $\phi(M)$. However, if $\phi(M)$ is modeled as a smooth function (e.g., a Schechter function), a stable solution is reached within 10 iterations.

2.2. *Combining $X(M, \sigma)$ Estimates to Obtain $\phi(M)$*

Each $X_i(M, \sigma)$ calculated above for each center galaxy should be an unbiased, albeit noisy, estimator of the quantity $\phi(M)\Xi(\sigma)$. We now wish to combine these estimates in an optimal way to obtain a close to minimum variance estimate of $\phi(M)$.

Again following Saunders et al., the expected variance in the quantity n_i is

$$\begin{aligned} \mathrm{Var}\,(n_i) \approx n_i' &[1 + p(m, \sigma, y)\phi(M)\Xi(\sigma)] \\ &\times [1 + \bar{N}(m)J_2(\theta)][1 + f\phi(M)J_3(\sigma)] \ , \end{aligned} \quad (9)$$

where

$$J_2(\theta) = 2\pi \int_0^\theta \theta' w(\theta') d\theta' \ , \quad (10)$$

and

$$J_3(\sigma) = 4\pi \int_0^\sigma \sigma'^2 \xi(\sigma') d\sigma' \ , \quad (11)$$

and f is the total fraction of galaxies with measured redshifts. In combining the individual measurements X_i to an overall estimate for $\phi(M)$, we sum over center galaxies, weighting each measurement by $b_i = [\Xi(\sigma)]^2/\mathrm{Var}\ (X_i)$,

$$\phi(M) = \frac{\sum_i b_i X_i/\Xi(\sigma)}{\sum_i b_i}\ , \tag{12}$$

$$\frac{1}{b_i} = \frac{1}{n_i'[p(m,\sigma,y)\Xi(\sigma)]^2}\,[1 + p(m,\sigma,y)\phi(M)\Xi(\sigma)] \times [1 + \bar{N}(m)J_2(\theta)][1 + f\phi(M)J_3(\sigma)]\ . \tag{13}$$

The expected variance on our final measure of $\phi(M)$ is then

$$\mathrm{Var}\ [\phi(M)] = 1/\sum_i b_i\ . \tag{14}$$

3. GALAXY SAMPLES AND APPLICATION

For center galaxies, we use the Stromlo-APM Redshift Survey (Loveday et al. 1996), which consists of 1787 galaxies with $b_J \leq 17.15$ selected randomly at a rate of 1 in 20 from the APM Galaxy Survey (Maddox et al. 1990a, 1990b). We count APM galaxies around each redshift survey galaxy in five linearly spaced bins of projected separation σ up to 5 h^{-1} Mpc and in 22 evenly spaced bins in apparent magnitude from $b_J = 15$ to 20.5. There are a total of 2,389,032 APM galaxies in this magnitude range. In order to correct for survey boundaries and holes drilled out around bright stars and large galaxies, we use a random catalog of 3,476,477 random points uniformly distributed over the area of the APM survey. Although there are only about 1.5 times as many random points as galaxies overall, the number of random points is significantly larger than the number of galaxies (527,611) in the faintest apparent magnitude bin. Thus, shot noise in the random catalog introduces negligible random error into our results.

When counting galaxy and random points in projection around center galaxies, we avoid objects within one major diameter of the center galaxy. This is to avoid three biases that might otherwise be caused by a large foreground galaxy: (1) obscuration of faint galaxies directly behind it, (2) lensing of background galaxies, and (3) breakup of a large galaxy by the APM machine into spurious subimages, artificially boosting the apparent number of projected neighbors. The worst of these latter cases have already been removed by the "holes" drilled around large images during the construction of the APM survey (Loveday 1996; Maddox et al. 1990a). The majority of galaxies in the Stromlo-APM survey have $\mu_{b_J} \approx 25$ isophotal major diameters of 20″–100″.

We assume a power-law form for the spatial correlation function, $\xi(r) = (r/r_0)^{-\gamma}$, with $\gamma = 1.71$ and $r_0 = 5.1\ h^{-1}$ Mpc (Loveday et al. 1995). The projected correlation function is then given by

$$\Xi(\sigma) = (\sigma/\sigma_0)^{1-\gamma}\ , \tag{15}$$

where

$$\sigma_0 = \left[r_0^{\gamma}\,\Gamma\left(\frac{1}{2}\right)\Gamma\left(\frac{\gamma-1}{2}\right)\Big/\Gamma\left(\frac{\gamma}{2}\right)\right]^{1/(\gamma-1)}\ . \tag{16}$$

For an initial luminosity function $\phi(M)$, we use the Schechter function fit from Loveday et al. (1992). We store the X_i calculated for each center galaxy by projected separation bin and *apparent* magnitude bin in order to avoid incompleteness effects that would otherwise result if we used *absolute* magnitude bins. We convert apparent to absolute magnitudes when we combine the X_i estimates in equation (12), using 22 bins in absolute magnitude from $M = -22$ to $M = -11$. At this stage, we also have the choice of which σ-bins to use; for example we can count galaxies at projected separation 0–1, 0–2, or 2–5 h^{-1} Mpc. The consistency of the estimates $\phi(M)$ for a range of projected separations will provide important confirmation of our results.

4. JUSTIFYING THE USE OF NEARBY CENTER GALAXIES

Before we present the results of this analysis, we first justify our assumption that excess faint galaxies seen close in projection to nearby redshift survey galaxies really are physically correlated. The APM galaxy survey has a magnitude limit of $b_J = 20.5$, corresponding to a limiting depth for L^* galaxies of $\sim 600\ h^{-1}$ Mpc, whereas galaxies of absolute magnitude $M_{B_J} = -15$ can only be seen out to a distance of $115\ h^{-1}$ Mpc. One might therefore wonder whether fluctuations in the number of uncorrelated background galaxies might swamp the contribution from genuinely correlated dwarf galaxies for nearby centers. We therefore perform a simple experiment to show that the number of APM galaxies counted to various magnitude limits is systematically larger close to a nearby center galaxy than in a random control field.

Taking in turn those $N_{\mathrm{cen}} = 477$ galaxies in the Stromlo-APM Survey that are closer than $100\ h^{-1}$ Mpc as centers, we count the number of APM galaxies (N_{gal}) within a projected separation of $1\ h^{-1}$ Mpc and also the number of background galaxies (N_{bgr}) within the same solid angle at a randomly chosen location. We use the random catalog to correct for solid angle lost due to the survey boundary and holes drilled out around large images. This is done for APM galaxies to a magnitude limit of $b_J = 20.0$, 19.0, 18.0, and 17.0. In Figure 1, we plot the frequency histograms (over the 477 center galaxies) of the ratio $N_{\mathrm{gal}}/N_{\mathrm{bgr}}$ (*solid histogram*) and its inverse $N_{\mathrm{bgr}}/N_{\mathrm{gal}}$ (*dotted histogram*). One can clearly see that the ratio $N_{\mathrm{gal}}/N_{\mathrm{bgr}}$ is systematically greater than unity, i.e., there is a statistical excess of APM galaxies near center galaxies. One can quantify this excess by measuring the mean and rms of the ratio $N_{\mathrm{gal}}/N_{\mathrm{bgr}}$ over centers. The mean and its standard error $[\sigma(N_{\mathrm{gal}}/N_{\mathrm{bgr}})/\sqrt{N_{\mathrm{cen}}}]$ are shown in Table 1. Also shown in this table is the probability from the Kolmogorov test that the quantities N_{gal} and N_{bgr} come from the same distribution. We see, particularly for the brighter magnitude cuts, that the distributions N_{gal} and N_{bgr} are significantly different, and that the ratio $N_{\mathrm{gal}}/N_{\mathrm{bgr}}$ is

TABLE 1

GALAXY COUNTS ABOUT CENTER GALAXIES N_{gal} AND CONTROL FIELDS N_{bgr}

m_{lim}[a]	$\langle N_{\mathrm{gal}}/N_{\mathrm{bgr}}\rangle$[b]	K-S Test[c]
a 20.0.....	1.08 ± 0.017	2.3×10^{-1}
b 19.0.....	1.16 ± 0.025	4.9×10^{-2}
c 18.0.....	1.35 ± 0.041	2.2×10^{-3}
d 17.0.....	1.90 ± 0.109	2.1×10^{-6}

[a] Magnitude limit of APM galaxies.
[b] Mean and standard error in the ratio $N_{\mathrm{gal}}/N_{\mathrm{bgr}}$.
[c] Probability that N_{gal} and N_{bgr} are drawn from the same distribution.

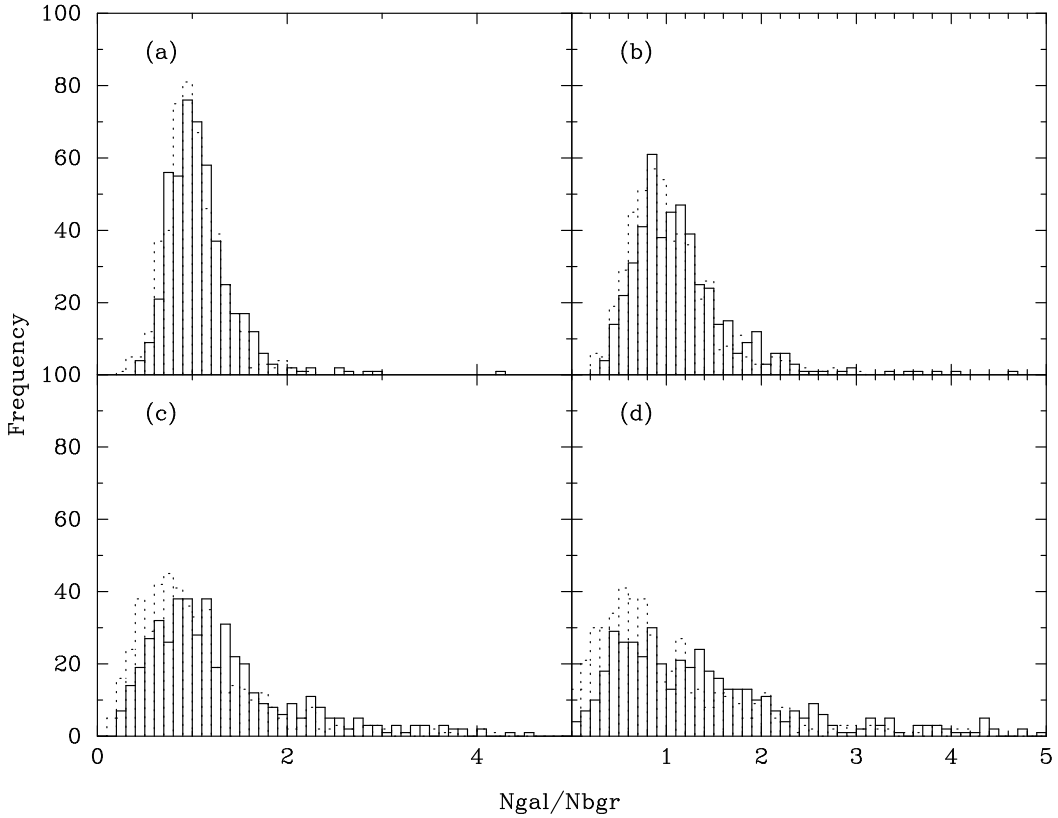

FIG. 1.—Plots of the ratio of APM galaxies counted around center galaxies (N_{gal}) over the number of APM galaxies in randomly placed control fields (N_{bgr}) of the same solid angle. The solid histogram shows the ratio N_{gal}/N_{bgr}, and the dotted histogram shows the inverse N_{bgr}/N_{gal}. APM galaxies were counted to a b_J magnitude limit of (*a*) 20.0, (*b*) 19.0, (*c*) 18.0, and (*d*) 17.0.

systematically larger than unity at at least the 4 σ level. From this test we conclude that we are justified in assuming that the excess APM galaxies seen close to Stromlo-APM center galaxies are physically correlated, even for center galaxies much closer than the characteristic depth of the APM galaxy survey.

5. RESULTS

In Figure 2*a* the points with error bars show the first-iteration estimate of the luminosity function $\phi(M)$, counting galaxies to projected separation $\sigma \leq 1\ h^{-1}$ Mpc. For comparison, this plot also shows (*solid line*) our earlier Schechter function fit to $\phi(M)$ using the redshift survey galaxies alone (Loveday et al. 1992) plus its extrapolation to lower luminosities (*dotted line*). Comparing with the earlier result, we see three regimes. (1) For $M \lesssim -18$, we see good agreement with the Schechter function. (2) For $-18 \lesssim M \lesssim -15$, we see that the new determination of $\phi(M)$ lies $\sim 2\ \sigma$ *below* the Schechter function. (3) At the faintest luminosities, $M \gtrsim -15$, we see a sharp rise in $\phi(M)$, rising well above the Schechter function. Thus, there appears to be a significant excess of faint galaxies above a flat faint-end power law, but we first need to understand why we disagree with our earlier estimate of $\phi(M)$ over the magnitude range $-18 \lesssim M \lesssim -15$.

We believe that this apparent discrepancy is due to the fact that we are really estimating the product $\phi(M)\Xi(\sigma)$ and we are assuming that $\Xi(\sigma)$, and therefore $\xi(r)$, is fixed, i.e., *independent of galaxy luminosity*. In fact, as we showed in an earlier paper (Loveday et al. 1995), there is evidence that low-luminosity galaxies are less strongly clustered than L^* ($M^* \approx -19.7$) galaxies, and thus we would expect our estimate of $\phi(M)\Xi(\sigma)$ to be biased low at low luminosities, as we indeed observe in Figure 2*a* over the magnitude range $-18 \lesssim M \lesssim -15$. This effect was also noted by Lorrimer et al. (1994) in their analysis of the distribution of satellite galaxies. The variation of clustering strength with luminosity is too poorly known to attempt to correct the $\phi(M)$ estimate shown here. In fact, the present data provides probably our best constraints on how $\xi(r)$ varies with luminosity.

By absolute magnitude $M \approx -14$ another effect is dominating: either the luminosity segregation reverses (such that $M \gtrsim -14$ galaxies are *more* strongly clustered about L^* galaxies than other L^* galaxies) and/or the intrinsic space density of dwarf galaxies is significantly higher than predicted by extrapolation of a flat faint-end Schechter function. As we will see below, the latter seems a more likely explanation for the observed excess of faint galaxies near $\sim L^*$ galaxies. It also has the attractive feature of helping to explain the observed steep number counts of faint galaxies compared with traditional no-evolution models.

Figure 2*a* showed our estimate of $\phi(M)$ after just one iteration, i.e., assuming that the true luminosity function is a flat faint-end Schechter function. Thus, the steep faint end is not due to an instability in our iteration procedure. Figure 2*b* shows our estimate of $\phi(M)$ after 10 iterations, by which time the solution has converged. We see that the faint-end slope has steepened slightly further. To model the observed $\phi(M)$, we have fitted a modified form of the Schechter func-

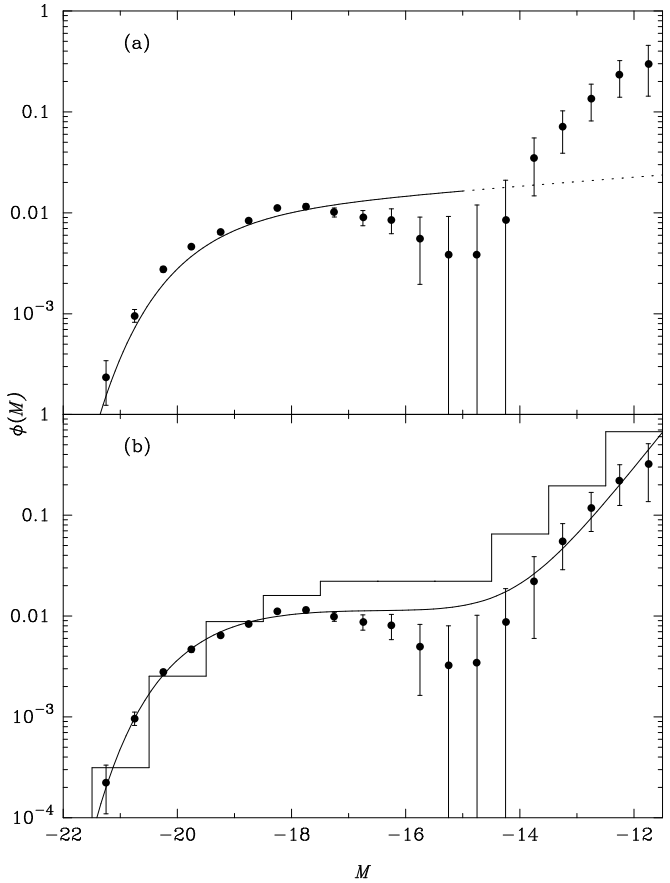

FIG. 2.—Estimates of the galaxy luminosity function $\phi(M)$. (*a*) After just one iteration. The solid line shows the earlier Schechter function fit to $\phi(M)$ using the redshift survey galaxies alone (Loveday et al. 1992); its extrapolation to lower luminosities is shown by the dotted line. (*b*) After 10 iterations, by which time the solution has converged. The smooth curve shows a "double power-law" Schechter fit (eq. [17]), and the histogram shows the Gronwall & Koo (1995) model.

tion, with an additional faint-end power law:

$$\phi(L) = \phi^*\left(\frac{L}{L^*}\right)^{\alpha} \exp\left(\frac{-L}{L^*}\right)\left[1 + \left(\frac{L}{L_t}\right)^{\beta}\right]. \qquad (17)$$

In this formulation ϕ^*, L^*, and α are the standard Schechter parameters, L_t is a transition luminosity between the two power laws and β is the power-law slope of the very faint end. No physical interpretation is intended by this choice of formula, it is merely a convenient way of modeling the observed $\phi(L)$ over this extended range of luminosity and for estimating the faint-end slope. The line in Figure 2*b* shows our best-fit "double power-law" luminosity function, which has parameters: $\alpha = -0.94$, $M^* = -19.65$, $\phi^* = 1.54 \times 10^{-2}\ h^{-3}$ Mpc^3, $M_t = -14.07$, and $\beta = -2.82$. Although this fit is poor over the range $-17 \lesssim M \lesssim -14$, our $\phi(M)$ estimate is almost certainly biased low over this range by the weaker clustering of galaxies fainter than L^*. Clearly, the faint-end slope $\beta = -2.82$ cannot extend to indefinitely low luminosities, but it shows no obvious signs of flattening brightward of $M = -12$.

6. CHECKS AND TESTS

6.1. *Varying Projected Separation σ*

In the preceding section we presented results based only on counts of neighboring galaxies at a projected separation of $\sigma \leq 1\ h^{-1}$ Mpc. By increasing σ one decreases shot-noise errors by increasing the total number of neighbors, although now a smaller fraction of these neighbors will be genuinely correlated with the center galaxy. Figure 3 shows our estimate of $\phi(M)$ if we count galaxies to a projected separation $\sigma \leq 2\ h^{-1}$ Mpc (*solid symbols*) and $\sigma \leq 5\ h^{-1}$ Mpc (*open symbols*). We see that the estimated $\phi(M)$ is insensitive to the limiting σ used, except that the deficit at $M \approx -15$ worsens as the maximum projected separation increases, and the error bars increase. This is to be expected from our earlier results on luminosity segregation, since Figure 6 of Loveday et al. (1995) shows that the weaker clustering of sub-L^* galaxies is more pronounced at scales larger than $1\ h^{-1}$ Mpc. The error bars also increase if we decrease the limiting projected separation to values of less than $1\ h^{-1}$ Mpc. Counting neighbors to $\sigma \approx 1\ h^{-1}$ Mpc, as shown in Figure 2, thus appears to be about optimal for this analysis.

6.2. *Varying Limiting Apparent Magnitude*

The second test we have performed is to cut back on the magnitude limit to which we count APM galaxies. There are two reasons for doing this. The first is that there is some indication that star-galaxy separation is slightly less reliable in the faintest half-magnitude slice of the APM survey than for brighter objects (Maddox et al. 1996). The second is to show that the poor match between volumes sampled by the bright redshift survey and the faint photometric survey does not lead to a systematic bias in the estimated luminosity function. In Figure 4 we plot the LF estimated by counting APM galaxies to 20th, 19th, 18th, and 17th magnitude, respectively. In each case, we see that the estimated LF is consistent with that estimated from the full $b_J < 20.5$ sample. Even cutting back the "faint" survey to $b_J < 17$ (actually slightly shallower than the redshift survey), we still see evidence for a steep faint end to the luminosity function. One should note that the signal contributing to the faint end of the LF is coming from decreasingly smaller volumes as one cuts back on the magnitude limit. A galaxy of absolute magnitude $M_{B_J} = -15$ can only be seen to distances of 93, 60, 39 and 25 h^{-1} Mpc, respectively, for galaxy samples cut to $b_J = 20.0$, 19.0, 18.0 and 17.0. The consistency of

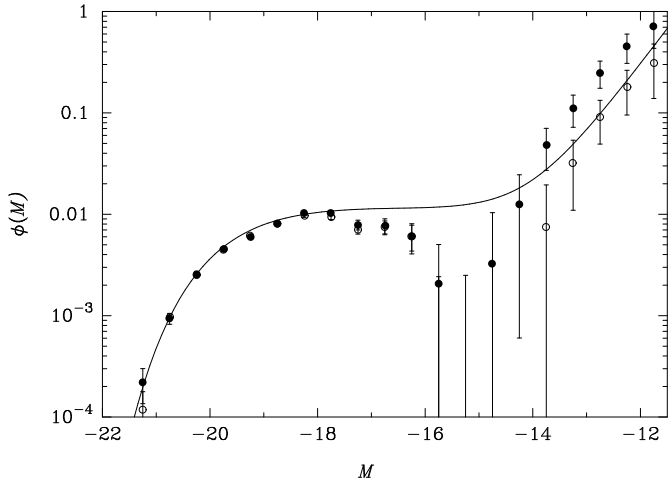

FIG. 3.—Estimates of the galaxy luminosity function $\phi(M)$ obtained by counting APM galaxies to a projected separation $\sigma \leq 2\ h^{-1}$ Mpc (*solid symbols*) and $\sigma \leq 5\ h^{-1}$ Mpc (*open symbols*). The smooth curve is the same "double power-law" Schechter fit shown in Fig. 2*b*.

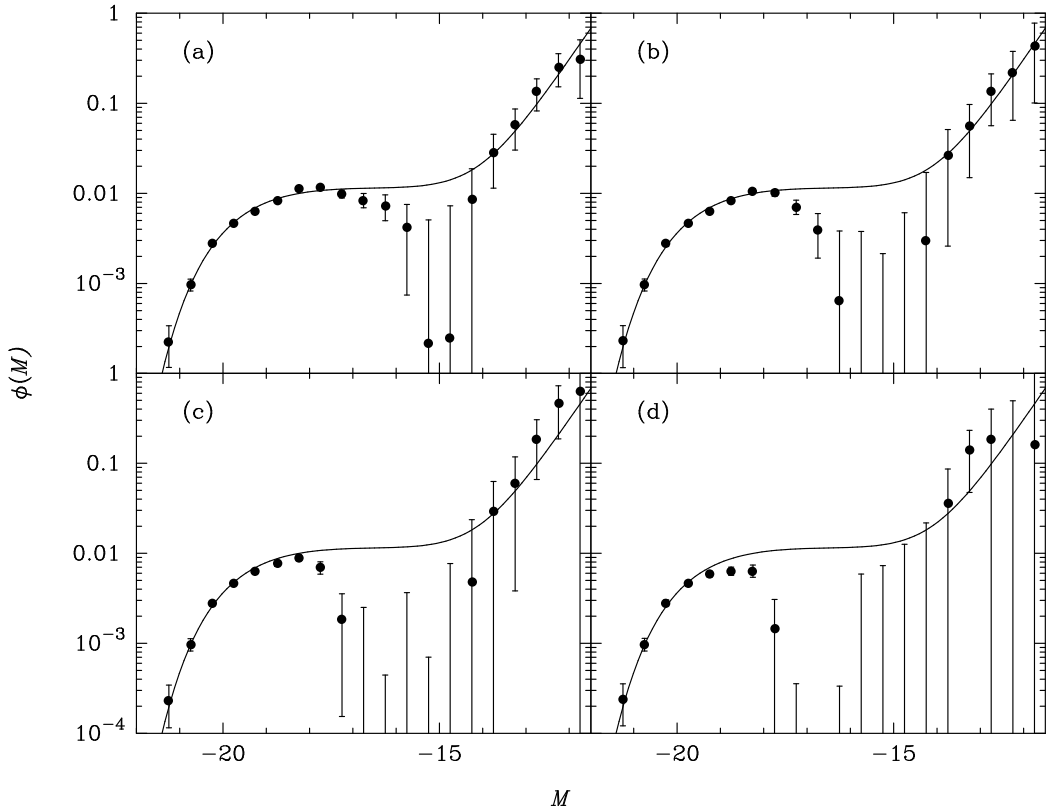

FIG. 4.—Estimates of the galaxy luminosity function $\phi(M)$ obtained by counting APM galaxies to a b_J magnitude limit of (*a*) 20.0, (*b*) 19.0, (*c*) 18.0, and (*d*) 17.0. The smooth curve is the same "double power-law" Schechter fit shown in Fig. 2*b*.

estimated faint-end slopes using galaxies over this range of volumes argues strongly against the observed steep faint-end slope being due to a "sampling" or "volume" effect.

6.3. *Analysis of Simulations*

As a further test of our methods, we have generated two sets of mock-APM surveys with known luminosity function and two-point correlation function, thus allowing us to check that we indeed are measuring the "true" luminosity function. The first set of simulations ("Sch") has galaxy luminosities drawn from a flat faint-end Schechter function ($\alpha = -1$, $M^* = -19.5$). The second set ("DP") has a "double power-law" function of the form (17) with parameters $\alpha = -1$, $M^* = -19.5$, $\beta = -2.6$, $M_t = -14.5$. The idea is to check that our method for estimating $\phi(M)$ can reliably distinguish between these two models.

For each model we generated five Soneira & Peebles (1978) hierarchical clustering simulations, each containing 2.4 million galaxies in the area of the APM survey. From each of these mock APM surveys, we formed mock Stromlo-APM Redshift Surveys by sampling one galaxy in 40 brighter than $b_J = 17.15$ at random. Note that the sparser sampling rate compared with the real data (1 in 20) is required to match the numbers of galaxies in the faint APM Galaxy Survey and the brighter redshift survey sample. This reflects the steep slope seen in the APM number counts by Maddox et al. (1990c) but not modeled in the simulations. The mock redshift surveys contained on average 1648 galaxies each, and the measured real space galaxy correlation function was well described on scales 1–20 h^{-1} Mpc by a power law with parameters $\gamma = 1.8$ and $r_0 = 4.9$ for the "double power-law" simulations, and with $\gamma = 1.8$ and $r_0 = 5.1$ for the Schechter function simulations, thus providing an excellent match to the observed real-space clustering of Stromlo-APM galaxies (Loveday et al. 1995).

We analyzed the simulations in the same way as the real data; counting galaxies in the mock-APM survey about center galaxies in the respective mock-Stromlo survey. In Figure 5*a* we plot the mean $\phi(M)$ measured from the five "DP" simulations as the symbols; the error bars show the 1 σ scatter between the realizations. These error bars are in good agreement with the errors estimated from equation (14). Also shown are the individual estimates (*dashed lines*) and the true luminosity function (*solid line*). We see that the mean estimated $\phi(M)$ is in reasonable agreement with the true LF: if anything we tend to *underestimate* the slope of the faint end of the luminosity function. We also see that estimates from the individual simulations can differ significantly from the true LF: two of the estimates show a *decrease* in $\phi(M)$ faintward of $M \approx -17$. This lack of robustness in the individual estimates of the LF is also apparent in Figure 5*b*, where we plot the results from the "Sch" simulations. Although the mean $\phi(M)$ is consistent with a flat faint end, and inconsistent with the double power-law function shown, two of the estimates do show an apparent rise above the expected flat faint-end slope. Neither, however, maintains the rise as faint as $M = -12$.

Overall, although individual simulations can show a wide deviation from the expected behavior, it seems that we are more likely to underestimate rather than overestimate the faint-end slope of the luminosity function, and hence the

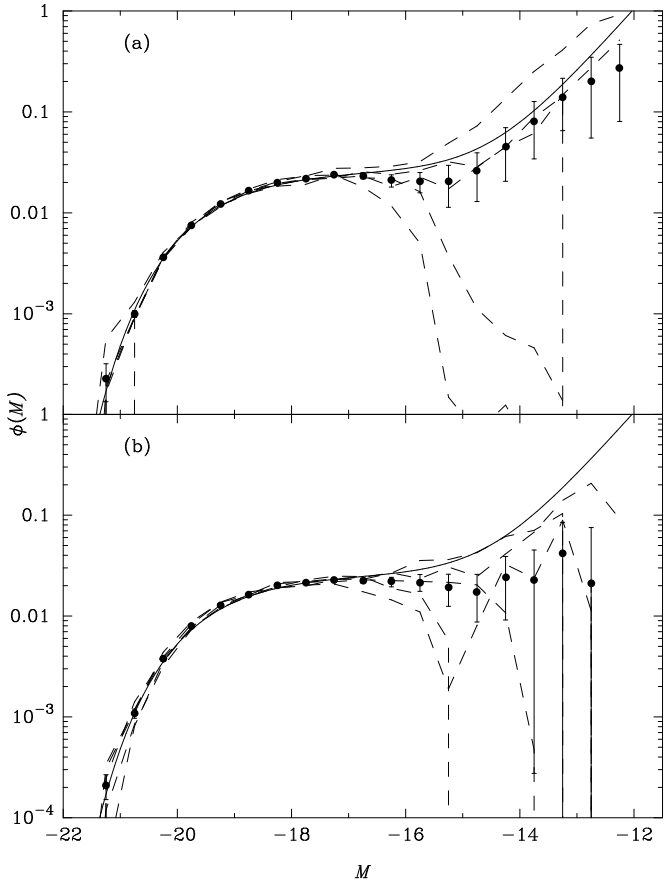

FIG. 5.—Analysis of simulations. The dashed lines show the individual realizations, the symbols with error bars show the mean and 1 σ fluctuations between them. The solid line shows the "double power-law" LF used in the "DP" simulations. (*a*) Results from the "double power-law" simulations (DP). (*b*) Results from Schechter function simulations (Sch).

space density of dwarf galaxies. Our estimated errors are in good agreement with the scatter between simulations.

7. CONCLUSIONS AND DISCUSSION

We have seen that the number of dwarf ($M \gtrsim -15$) galaxies seen close in projection on the sky to $\sim L^*$ galaxies ($-22 \lesssim M \lesssim -15$) is much larger than expected for a flat faint-end Schechter function and for the standard galaxy correlation function ($\gamma \approx 1.7$, $r_0 \approx 5\ h^{-1}$ Mpc). We may thus infer that the space density of galaxies rises sharply above a flat faint-end Schechter function for $M \gtrsim -15$ and/or that the clustering of dwarf galaxies around $\sim L^*$ galaxies is much stronger than the autocorrelation function of $\sim L^*$ galaxies. An extreme case of the latter explanation might be that dwarf galaxies *only* exist close to $\sim L^*$ galaxies.

It is no easy matter to determine which (or both) of these explanations is correct. Since all of the $M \gtrsim -15$ dwarf galaxies must lie within $y \lesssim 115\ h^{-1}$ Mpc to be visible in the APM survey, even if there is a generally higher space density of dwarfs, they have a relatively minor ($\sim$20%) effect on total predicted number counts in the survey. However, one can place a lower limit on the space density of dwarf galaxies by making the extreme assumption that they only exist close to $\sim L^*$ galaxies. In fact, in Figure 3, we see an excess of dwarf galaxies up to a projected separation of at least $5\ h^{-1}$ Mpc from $\sim L^*$ galaxies. Thus, a lower limit may be estimated by assuming that they occur with the measured space density only within $5\ h^{-1}$ Mpc of an $\sim L^*$ galaxy. The lower limit on the average mean density of dwarf galaxies is then given by multiplying their measured space density by the fraction of space within $5\ h^{-1}$ Mpc of an $\sim L^*$ galaxy.

In order to estimate the filling factor of $\sim L^*$ galaxies in the local universe, we have generated another set of five Soneira-Peebles simulations within a cubic volume $100\ h^{-1}$ Mpc on a side and without applying a selection function. These simulations contain 47,000 galaxies each, and thus their space density is $\bar{n} = 4.7 \times 10^{-2}\ h^3$ Mpc^{-3}, as measured for $\sim L^*$ galaxies in the Stromlo-APM survey (Loveday et al. 1992). Additionally, the two-point correlation function of galaxies in these simulations is set to be well fitted by a power law with $\gamma = 1.82 \pm 0.06$ and $r_0 = 5.0 \pm 0.2$, in good agreement with the clustering measured by Loveday et al. (1995). Given these simulations, it is then simple to perform a Monte Carlo calculation of the volume inside each cube within $5\ h^{-1}$ Mpc of an $\sim L^*$ galaxy. We find that this factor lies in the range 0.57–0.62, i.e., a randomly chosen point in space has a 60% chance of lying within $5\ h^{-1}$ Mpc of one or more $\sim L^*$ galaxies. Now, integrating the luminosity function plotted in Figure 2*b* between $M = -15$ and -12 yields a measured density of dwarf galaxies of $\bar{n} \approx 0.20\ h^3$ Mpc^{-3}. Correcting this by the extreme assumption that dwarf galaxies are only found within $5\ h^{-1}$ Mpc of an $\sim L^*$ galaxy results in a *lower limit* on the space density of dwarf galaxies of $\bar{n} \approx 0.12\ h^3$ Mpc^{-3}. This is a factor of 2 higher than the density $\bar{n} \approx 0.058\ h^3$ Mpc^{-3} inferred from the $\alpha = -1.11$ Schechter function fit by Loveday et al. (1992).

In fact, the true space density of dwarf galaxies is likely to be significantly higher than this, for a number of reasons. First, our estimator assumes that galaxy clustering is independent of luminosity, whereas we know that sub-L^* galaxies are less strongly clustered than more luminous galaxies (e.g., Loveday et al. 1995). If this luminosity segregation extends to dwarf galaxies, then we will have underestimated their space density. Second, analysis of simulations (§ 6.3) shows that our estimator tends to underestimate the faint-end slope of $\phi(M)$ slightly, possibly due to a Malmquist-type bias. Third, as discussed by numerous authors, most galaxy surveys are likely to be missing a substantial fraction of low surface brightness galaxies, many of which will be dwarfs. For example, Sprayberry et al. (1997) find a pronounced upturn in the luminosity function for their sample of low surface brightness galaxies. Thus, we regard our above estimate of the space density of dwarf galaxies, $\bar{n} \approx 0.12\ h^3$ Mpc^{-3}, as a *lower limit* on the true value.

A high space density of dwarf galaxies, assuming that they are predominantly late-type, blue galaxies, which suffer smaller K-correction dimming than redder, early-type galaxies, provides a natural explanation for the steep observed number counts of faint galaxies. Evidence for a large contribution from late-type galaxies to the faint galaxy counts in the *HST* Medium Deep Survey has been presented by Driver, Windhorst, & Griffiths (1995). Zucca et al. (1997) have found that the luminosity function for emission-line galaxies (ELGs) is significantly steeper at the faint end than the LF for non-ELGs, also supporting the hypothesis that the faint end of the galaxy LF is dominated by late-type

galaxies. Gronwall & Koo (1995) were able to match observations of galaxy number counts in the K, R, and B_J bands, as well as color and redshift distributions, for a mild evolution model by assuming that the faint end of the galaxy luminosity function is dominated by blue galaxies ($B-V \leq 0.6$) and rises significantly above a Schechter function with flat faint-end slope. We plot the Gronwall & Koo model total luminosity function in Figure 2*b*, and we see remarkably good agreement with our observations. Our results thus support the model of Gronwall & Koo; there is no need to invoke exotic forms of galaxy evolution to explain observed galaxy number counts at faint magnitudes.

It is a pleasure to thank my colleagues George Efstathiou, Steve Maddox, Bruce Peterson and Will Sutherland, who made the APM and Stromlo-APM surveys possible. The simulations used in this paper were carried out using computing facilities at the Fermi National Accelerator Laboratory. The referee, Chris Impey, is thanked for his comments, which have (hopefully) helped make these results more convincing.

REFERENCES

Babul, A., & Rees, M. J. 1992, MNRAS, 255, 346
Broadhurst, T. J., Ellis, R. S., & Glazebrook, K. 1992, Nature, 355, 55
Broadhurst, T. J., Ellis, R. S., & Shanks, T. 1988, MNRAS, 235, 827
Cowie, L. L., Songaila, A., & Hu, E. M. 1991, Nature, 354, 460
Driver, S. P., Windhorst, R. A., & Griffiths, R. E. 1995, ApJ, 453, 48
Eales, S. 1993, ApJ, 404, 51
Ellis, R. S. 1987, in in IAU Symp. 124, Observational Cosmology, ed. A. Hewitt et al. (Dordrecht: Reidel), 367
Fukugita, M., Takahara, F., Yamashita, K., & Yoshii, Y. 1990, ApJ, 361, L1
Gronwall, C., & Koo, D. C. 1995, ApJ, 440, L1
Koo, D. C., Gronwall, C., & Bruzual A.,G. 1993, ApJ 415, L21
Koo, D. C., & Kron, R. G. 1992, ARA&A, 30, 613
Lilly, S. J. 1993, ApJ, 411, 501
Lonsdale, C. J., & Chokshi, A. 1993, AJ, 105, 1333
Lorrimer, S. J., Frenk, C. S., Smith, R. M., White, S. D. M., & Zaritsky, D. 1994, MNRAS, 269, 696
Loveday, J. 1996, MNRAS, 278, 1025
Loveday, J., Maddox, S. J., Efstathiou, G., & Peterson, B. A. 1995, ApJ, 442, 457
Loveday, J., Peterson, B. A., Efstathiou, G., & Maddox, S. J. 1992, ApJ, 390, 338
Loveday, J., Peterson, B. A., Maddox, S. J., & Efstathiou, G. 1996, ApJS, 107, 201
Maddox, S. J., Efstathiou, G., & Sutherland, W. J. 1990a, MNRAS, 246, 433
———. 1996, MNRAS, 283, 1227
Maddox, S. J., Sutherland, W. J. Efstathiou, G., & Loveday, J. 1990b, MNRAS, 243, 692
Maddox, S. J., Sutherland, W. J. Efstathiou, G., Loveday, J., & Peterson, B. A. 1990c, MNRAS, 247, 1P
Marzke, R. O., Huchra, J. P., & Geller, M. J. 1994, ApJ, 428, 43
Phillipps, S., & Shanks, T. 1987, MNRAS, 227, 115
Saunders, W., Rowan-Robinson, M., & Lawrence, A. 1992, MNRAS, 258, 134
Schechter, P. L. 1976, ApJ, 203, 297
Soneira, R. M., & Peebles, P. J. E. 1978, AJ, 83, 845
Sprayberry, D., Impey, C. D., Irwin, M. J., & Bothun, G. D. 1997, ApJ, 482, 104
Takamiya, M., & Kron, R. G. 1995, AJ, 110, 1083
White, S. D. M. 1989, MNRAS, 237, 51
Zucca, E., et al. 1997, A&A, 326, 477